A Disk of Scattered Icy Objects and the Origin of Jupiter-Family Comets

Martin J. Duncan and Harold F. Levison

Orbital integrations carried out for 4 billion years produced a disk of scattered objects beyond the orbit of Neptune. Objects in this disk can be distinguished from Kuiper belt objects by a greater range of eccentricities and inclinations. This disk was formed in the simulations by encounters with Neptune during the early evolution of the outer solar system. After particles first encountered Neptune, the simulations show that about 1 percent of the particles survive in this disk for the age of the solar system. A disk currently containing as few as $\sim 6 \times 10^8$ objects could supply all of the observed Jupiter-family comets. Two recently discovered objects, 1996 RQ_{20} and 1996 TL_{66}, have orbital elements similar to those predicted for objects in this disk, suggesting that they are thus far the only members of this disk to be identified.

The 160 discovered comets that are dynamically controlled by Jupiter [called Jupiter-family comets or JFCs (*1*)] are short-lived, implying that they must be resupplied from some external reservoir. The current working hypothesis is that JFCs originate in the Kuiper belt—a disk of objects beyond the orbit of Neptune in nearly-circular orbits that have remained largely unchanged since the formation of the outer planets (*2–4*). In this scenario, weak dynamical instabilities and collisions acting on billion-year time scales cause a steady influx of objects from the region between 30 and 50 astronomical units (AU) (*5*). Numerical integrations of this influx show that the orbital element distribution of the resulting objects that would become active comets is indistinguishable from the orbital element distribution of observed JFCs (*6, 7*). Based on the total number of known JFCs and the assumption that dynamical sculpting was the only important process in the Kuiper belt's evolution, these simulations suggest that there are currently $\sim 7 \times 10^9$ objects in the Kuiper belt that have not encountered Neptune and remain in low to moderately eccentric orbits within 50 AU of the sun.

The short median dynamical lifetime ($\sim 5 \times 10^7$ years) of objects that leave the Kuiper belt and encounter Neptune (*6*) has often been taken to imply that Kuiper belt replenishment is required to maintain the observed population of JFCs. However, in integrations of objects subsequent to their first Neptune encounter (*6*), we found that about 5% of the objects survived the length of the integration (10^9 years). This suggests that replenishment from the Kuiper belt might not be required if a sufficiently large fraction of objects scattered by Neptune survived for the age of the solar system. Here, we investigate the possibility that all of the current JFCs originated in a remnant disk of scattered, icy objects (SIOs) that first encountered Neptune during the early dynamical evolution of the outer solar system. Although such a disk was previously suggested as the source of the JFCs (*8*), our simulations model the dynamical formation and evolution of this disk more accurately, producing a detailed model of temporal variations and orbital element distribution for SIOs that can be compared with observations (*9*).

Because our earlier integrations (*6*) lasted for only a billion years, the first step was to extend those calculations to 4 billion years—roughly the age of the solar system. Our original integrations started with 2200 massless particles in Neptune-encountering orbits with semi-major axes (*a*) between 34 and 50 AU. We found that on billion-year time scales the number of particles remaining in the simulation was inversely proportional to time. In particular, 1% of the particles remained after 4 billion years. Some of the long-lived particles were scattered to long-period orbits (orbital periods $\gtrsim 10^4$ years) where encounters with Neptune became infrequent. However, at any time, 56% of the particles had orbits within 100 AU. The longevity of the particles within 100 AU is due in large part to their being temporarily trapped in or near mean-motion resonances with Neptune [Fig. 1 and (*10*)]. As a result, the distribution of *a* for the particles is peaked near many of the mean motion resonances with Neptune. In some cases, the longevity is enhanced by the presence of the Kozai resonance (*11*). In addition, all of the long-lived particles have their perihelion distances increased so that close encounters with Neptune no longer occur. Frequently, the increase in perihelion distance is associated with trapping in a mean motion resonance, although in many cases we have not been able to identify the exact process that was involved. On rare occasions, the perihelion distance can become as large as 48 AU, but 81% of the particles have perihelia between 32 and 36 AU.

We can estimate an upper limit on the number of possible SIOs by assuming that they are the sole source of the JFCs. Assuming that all the particles first encountered Neptune at the beginning of the 4-billion-year simulation, we computed the distribution of particles throughout the solar system at the current epoch (averaged over the last billion years for better statistical accuracy). The ratio of SIOs to visible JFCs (*12*) is

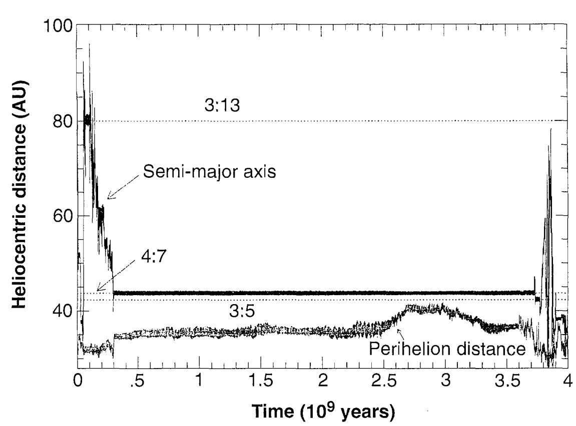

Fig. 1. The temporal behavior of a long-lived member of the disk of scattered objects. The black curve shows the behavior of the particle's semi-major axis. The gray curve shows the perihelion distance. The three dotted curves show the location of the 3:13, 4:7, and 3:5 mean motion resonances with Neptune. This particle initially underwent a random walk in semi-major axis due to encounters with Neptune. At about 7×10^7 years it was temporarily trapped in Neptune's 3:13 mean motion resonance for about 5×10^7 years. It then performed a random walk in semi-major axis until about 3×10^8 years when it was trapped in the 4:7 mean motion resonance, where it remained for 3.4×10^9 years. Notice the increase in the perihelion distance near the time of capture. While trapped in this resonance, the particle's eccentricity became as small as 0.04. After leaving the 4:7, it was trapped temporarily in Neptune's 3:5 mean motion resonance for $\sim 5 \times 10^8$ years and then went through a random walk in semi-major axis for the remainder of the simulation.

M. J. Duncan, Department of Physics, Queen's University, Kingston, Ontario K7L 3N6, Canada. E-mail: duncan@astro.queensu.ca
H. F. Levison, Space Science Department, Southwest Research Institute, Boulder, CO 80302, USA. E-mail: hal@gort.boulder.swri.edu

1.3×10^6. Because we estimate that there are currently 500 visible JFCs (*13*), there are $\sim 6 \times 10^8$ SIOs if they are the sole source of the JFCs (Fig. 2). For SIOs in the disk with $a < 50$ AU, eccentricities (e) from 0 to 0.3 are expected, while for those with $a > 50$ AU the eccentricities are greater and the range is narrower, consistent with elongated orbits with perihelia between 30 to 40 AU (Fig. 3). The inclinations (i) lie in the range from 0 to 30° for the SIOs with $a < 100$ AU (Fig. 3).

We can compare the orbital element distribution of SIOs with models of the Kuiper belt to determine whether real objects are Kuiper belt objects (KBOs) or SIOs. For the current orbital element distribution of KBOs, we refer to a planetary migration model (*14*) rather than to observations, because the model has information about regions of the Kuiper belt (particularly regions beyond 50 AU) where objects have not yet been observed (*15*). The migrating planet model of the Kuiper belt (*14*) is motivated by the 21 KBOs with well-determined orbits (*15*). The 21 KBOs (*15*) fall into two classes. Inside of ~41 AU, they are in mean motion resonances with Neptune and have $0.1 \lesssim e \lesssim 0.3$. Beyond ~41 AU they tend not to be in mean motion resonances and most have $e < 0.1$. The 21 KBOs have $a < 50$ AU and all but 3 have $i < 10°$. These observations are probably best explained by the planetary migration model in which Uranus and Neptune migrate outward during the final phases of their formation (*14*). This model matches many of the orbital properties of the observed KBOs, including the tendency for objects to be in mean motion resonances. It predicts $e = 0$ to 0.3 and $i = 0$ to 15° (Fig. 3).

A comparison between this model and our model of the distribution of SIOs shows that the two models overlap (Fig. 3). However, there are regions with large eccentricities, large inclinations, or both that we predict should be populated by SIOs that should not be populated by KBOs.

The existence of a disk of scattered objects is strongly suggested by the discoveries of two likely members, 1996 RQ_{20} and 1996 TL_{66}. 1996 RQ_{20} was discovered in September 1996 by E. Helin, D. Brown, and D. Rabinowitz and its orbital characteristics indicate $a = 47$ AU, $e = 0.3$, and $i = 32°$ (*16*). This object may have been scattered by Neptune and then captured in the 1:2 mean motion resonance with Neptune. We often see this behavior in the long-lived particles in our simulations. Indeed, this dynamical history could naturally explain the large i of this object, while other known mechanisms, such as migrating planets (*14*), do not give rise to such large inclinations (Fig. 3). 1996 TL_{66}, discovered by C. Trujillo *et al.* (*17*), is currently believed to have $a = 84$ AU, $e = 0.58$, and $i = 24°$, which implies a perihelion distance of 35 AU. This object is dynamically similar to the simulated disk of SIOs (Fig. 3). The a of this object is near the 2:9 mean motion resonance with Neptune, which is consistent with our results that most of the simulated SIOs lie near or in mean motion resonances.

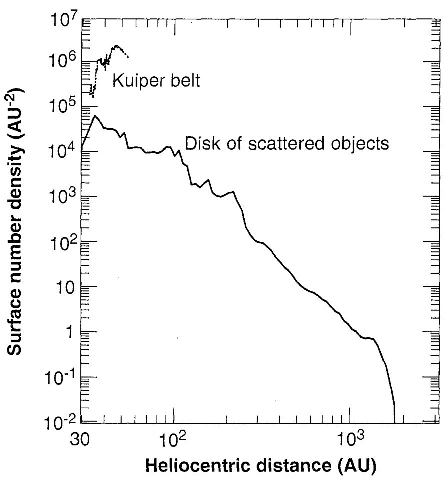

Fig. 2. The surface density (number of objects/AU^2) of objects beyond Neptune for two different models of the source of JFCs. The dotted curve is a model assuming that the Kuiper belt is the current source (*6*). There are 7×10^9 comets in this distribution between 30 and 50 AU. This curve ends at 50 AU because the models are unconstrained beyond this point and not because we believe that there are no objects there. The solid curve is our model assuming the disk of scattered objects is the sole source of the JFCs. There are currently 6×10^8 particles in this distribution.

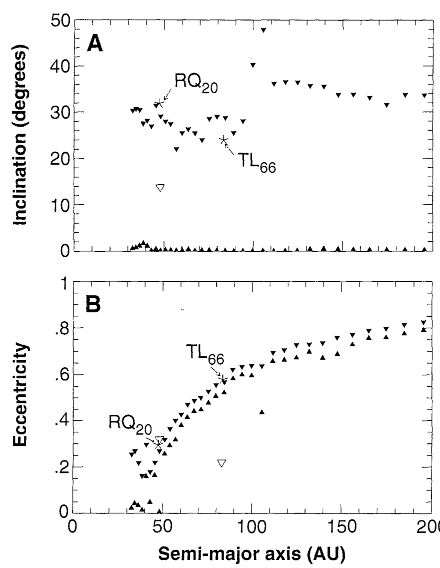

Fig. 3. The filled triangles show the range of (**A**) inclinations and (**B**) eccentricities predicted by our disk of scattered objects model as a function of semi-major axis. The upright and inverted triangles represent lower and upper limits, respectively. The open triangles represent upper limits as predicted by a migrating planet model of the Kuiper belt (*14*). The asterisks show the values for the two recently discovered trans-neptunian objects (*16*, *17*), which are labeled.

We can also estimate the size distribution of the SIOs. For large objects (radii ~ 100 km), two of the 23 trans-neptunian objects with well-known orbits detected in ground-based surveys (*15*) may be SIOs. These surveys suggest that there are 70,000 KBOs (*18*) with sizes greater than 50 km that are currently within 50 AU. Thus, we would expect there to be roughly 6100 comparably sized SIOs in the same region (*19*). For smaller objects (radii ~ 1 to 10 km, which is similar to the size range estimated for JFCs) our model predicts that ~23% of SIOs ($\sim 1.4 \times 10^8$ objects) lie between 30 and 50 AU. A single power-law differential size distribution can be fit to these populations, with the main uncertainty being the "typical" size of a comet. If the smallest detectable JFC is about 2 km, then the power law index is −4.2. For a JFC with a radius of 1 km, the index is −3.6. These values are uncertain, but lie near the range found for Kuiper belt cometary size distributions (*20*).

We should note some limitations of our simulations. We have assumed that the planets remained in their current configuration during the integration. However, as mentioned above, Uranus and Neptune may have migrated outward as they formed (*21*). Most of our particles survived for billions of years because they had their perihelion distances raised beyond the reach of Neptune, but an outwardly migrating Neptune may have caught up with these particles, reducing their lifetimes. However, models of the migration of Neptune (*21*) show that the movement most likely happened quickly (on the order of a few tens of millions of years), so the disk may have formed after Neptune stopped migrating. Alternatively, the migration of Neptune may have pushed the perihelion distances of the particles outward with it. The second caveat involves collisions between KBOs and SIOs. Recent numerical simulations show that if the early Kuiper belt was massive (containing a few Earth masses of objects), then collisions would have been common (*22*). Collisions could destroy objects or knock them out of the mean motion resonances with Neptune and thus could affect our estimate of the amount of material in the disk of SIOs.

Finally, we note that a disk of SIOs is a natural consequence of models of outer solar system formation. We found above that

~1% of the objects in the scattered disk remain after 4 billion years, and that 6×10^8 comets are currently required. Thus, we require an initial population of only 6×10^{10} comets [~0.4 Earth masses (*23*)] on Neptune-encountering orbits. Because planet formation is unlikely to have been 100% efficient, the original disk could have resulted from the scattering of even a small fraction of the tens of Earth masses of cometary material that must have populated the outer solar system in order to form Uranus and Neptune.

REFERENCES AND NOTES

1. See H. F. Levison in *Completing the Inventory of the Solar System*, T. W. Rettig and J. M. Hahn, Eds. (Astronomical Society of the Pacific, San Francisco, 1996), p. 173. To be precise, a JFC is defined to have a Tisserand parameter, *T*, with respect to Jupiter of between 2 and 3. The encounter velocity is $v_J\sqrt{3-T}$, where v_J is the mean orbital velocity of Jupiter around the sun. JFCs typically have semi-major axes < 7 AU and perihelion distances less than 3 AU. Their mean inclination is ~10°.
2. J. Fernández, *Mon. Not. R. Astron. Soc.* **192**, 481 (1980).
3. K. E. Edgeworth, *J. Br. Astron. Assoc.* **53**, 181 (1943); *Mon. Not. R. Astron. Soc.* **109**, 600 (1949); G. Kuiper, in *Astrophysics: A Topical Symposium*, J. A. Hynek, Ed. (McGraw Hill, New York, 1951), p. 357.
4. M. J. Duncan, T. R. Quinn, S. Tremaine, *Astrophys. J.* **328**, L69 (1988); T. R. Quinn, S. Tremaine, M. J. Duncan, *ibid.* **355**, 667 (1990).
5. H. F. Levison and M. J. Duncan, *Astrophys. J.* **406**, L35 (1993); M. Holman and J. Wisdom, *Astron. J.* **105**, 1987 (1993); M. J. Duncan, H. F. Levison, M. S. Budd, *ibid.* **110**, 3073 (1995).
6. H. F. Levison and M. J. Duncan, *Icarus*, in press.
7. A Kolmogorov-Smirnov test shows that the probability that the two distributions are derived from the same parent distribution is greater than 90% if the particles have physical lifetimes of ~12,000 years.
8. J. A. Fernandez and W.-H. Ip, *Icarus* **54**, 377 (1983); M. V. Torbett, *Astron. J.* **98**, 1477 (1989).
9. Once SIOs are perturbed inward by Neptune, they are dynamically indistinguishable from KBOs because an SIO and a KBO will have similar Tisserand parameters with respect to Neptune. Thus, it is not possible to distinguish between the two sources based on the dynamics of the JFCs alone. However, M. F. A'Hearn *et al.* [*Icarus* **118**, 223 (1995)] have shown that there are two distinct populations of JFCs based on chemical abundances. Perhaps this indicates that there are two different source for the JFCs.
10. This behavior can also be seen in figure 5 of M. Holman and J. Wisdom, *Astron. J.* **105**, 1987 (1993). This earlier work demonstrates that the basic processes of temporary capture into mean motion resonance are not dependent upon the details of how we integrated close encounters in our simulation.
11. To first order, the orbit of a particle has two precessions associated with it. The first is the precession of the location where the orbit crosses the plane of the solar system (known as node-crossing). The second is the precession of the longitude of perihelion. The Kozai resonance [Y. Kozai, *Astron. J.* **67**, 591 (1962)] occurs when the rate of these two precessions are the same. When a particle is in the Kozai resonance, it generally will not cross the plane of the solar system when it is at perihelion. Thus, particles with perihelion distances near Neptune will be protected from encounters with Neptune by the Kozai resonance.
12. We define a "visible" JFC as one with a perihelion distance < 2.5 AU. See (*6*) above for more details.
13. The observed population of JFCs suffers from observational biases, particularly with regard to a comet's perihelion distance and absolute magnitude. To perform a comparison between the results of our simulations and observations, we must correct for observational selection effects. A complete analysis is beyond the scope of this paper and we adopt the results in (*6*).
14. R. Malhotra, *Astron. J.* **110**, 420, (1995).
15. Currently, 42 trans-neptunian objects have been discovered from the ground (see http://cfa-www.harvard.edu/cfa/ps/lists/TNOs.html for a current list). Of those, 23 have been observed long enough and often enough to have well-determined orbits. The rest have not been observed enough, either because they are recently discovered or have been lost. Of those with good orbits, we categorize all but 1996 RQ_{20} and 1996 TL_{66} as KBOs.
16. E. Helin, D. Brown, D. Rabinowitz, *Minor Planet Electron. Circ. B19* (1997).
17. C. Trujillo *et al.*, *ibid. B18* (1997); J. Luu *et al.*, *Nature*, **387**, 573 (1997).
18. D. Jewitt, J. Luu, J. Chen, *Astron. J.* **112**, 1225, (1997).
19. This estimate is uncertain because the survey that found 1996 TL_{66} (*17*) had a different limiting magnitude and covered a different area of the sky than (*18*)
20. For a review, see P. R. Weissman and H. F. Levison, in *Pluto*, D. J. Tholen and S. A. Stern, Eds. (University of Arizona Press, Tucson, in press).
21. J. A. Fernandez and W.-H. Ip, *Icarus* **58**, 109 (1984).
22. S. A. Stern, *Astron. J.* **110**, 856 (1995); D. R. Davis and P. Farinella, *Icarus* **125**, 50 (1997).
23. We adopt an average mass of a comet of 6×10^{-12} Earth masses [P. R. Weissman, *Geol. Soc. Am. Spec. Pap.* **247**, 263 (1990)]. This value is uncertain, because the size distribution is poorly determined.

24. We are grateful to S. Tremaine, who motivated this line of inquiry. We also thank L. Dones, B. Marsden, A. Stern, B. Gladman, M. Holman, W. Merline, and P. Weissman for comments on this manuscript. H.F.L. acknowledges grants provided by the NASA Origins of Solar Systems and Planetary Geology and Geophysics Programs. M.J.D. is grateful for the continuing financial support of the Natural Science and Engineering Research Council of Canada and for financial support for work done in the U.S. from NASA Planetary Geology and Geophysics Programs. We also acknowledge funding for our computer equipment from the National Science Foundation and the Southwest Research Institute.

3 February 1997; accepted 16 May 1997

Paleobotanical Evidence for High Altitudes in Nevada During the Miocene

Jack A. Wolfe,* Howard E. Schorn, Chris E. Forest, Peter Molnar

Leaf physiognomy provides estimates of environmental parameters, including mean annual enthalpy, which is a thermodynamic parameter of the atmosphere that varies with altitude. Analyses of 12 mid-Miocene floras from western Nevada indicate that this part of the Basin and Range Province stood ~3 kilometers above sea level at 15 to 16 million years ago, which is 1 to 1.5 kilometers higher than its present altitude. Much, if not all, of the collapse to present-day altitudes seems to have been achieved by ~13 million years ago. The crust in much of this area has been extended and thinned throughout the past 40 to 50 million years, and the isostatic balance of a thinning crust requires subsidence, not uplift as suggested by previous paleobotanical work.

Terrestrial plants are generally regarded as highly responsive to environmental changes, and thus fossil plants offer one of the best methods for inferring paleoenvironmental parameters (*1*). In one approach, the environmental tolerances of a fossil species were assumed to be the same as those of its nearest living relative. Because in this method it was assumed that plants do not evolve by adapting to different environments (*2*), conclusions based on this method must—to varying degrees—be doubtful. Paleobotanical data using this nearest living relative method have been interpreted to indicate that most of the Basin and Range Province of Nevada was at low altitudes (<1 km) until <5 million years ago (Ma), when uplift is inferred to have started, which resulted in the ~1- to 1.5-km present-day mean altitudes of the basins (*3*). These estimates have been used as boundary conditions in numerical models of global climate during the Cenozoic, and it has been suggested that recent uplift helped initiate late Cenozoic glaciation (*4*). A second paleobotanical method relates the general physiognomy of plants to the environment, a relation that has generally been assumed to be valid, both today and in the past (*1*). In particular, gross physical aspects of leaves, including outlines, shapes, and sizes that can be readily observed on fossilized leaves, can be observed to change along present-day environmental gradients (*5*).

To calibrate changes in foliar physiognomy with changes in environmental parameters, leaves of at least 20 species of woody dicotyledons were collected close to meteorological recording stations (*5*), primarily in North America and the Caribbean region from latitudes 18°N to 62°N. Included in the sampling was vegetation ranging

J. A. Wolfe, Department of Geosciences, University of Arizona, Tucson, AZ 85721, USA.
H. E. Schorn, Museum of Paleontology, University of California, Berkeley, CA 94720, USA.
C. E. Forest and P. Molnar, Department of Earth, Atmospheric, and Planetary Sciences, Massachusetts Institute of Technology, Cambridge, MA 02139, USA.

*To whom correspondence should be addressed. E-mail: jwolfe@geo.arizona.edu